Proceedings of ISFOG 2025
5TH INTERNATIONAL SYMPOSIUM ON
FRONTIERS IN OFFSHORE GEOTECHNICS
Nantes, France | June 9-13 2025

ISBN 978-2-85782-758-0

Novel CPT-based p-y model for monopiles under lateral loads in sand

Zhentao LIU
Southeast University, Nanjing, China
Youhu ZHANG
Southeast University, Nanjing, China

ABSTRACT: A database of 26 high quality field lateral pile load tests from four independent studies is established. Based on the collected database, a CPT-based *p-y* model with a modified hyperbolic formulation is proposed. The model features four parameters, namely the initial soil-pile interaction stiffness (k_{ini}), the ultimate soil resistance (p_u), the stiffness degradation coefficient (m), and the ultimate soil resistance adjustment coefficient (A), which are all functions of the CPT cone tip resistance (q_c). The model is demonstrated to provide satisfactory performance in predicting the lateral response of monopiles in sand.
Keywords: Monopile; CPT; *p-y* model; offshore wind turbine

1 INTRODUCTION

Currently, the design of large diameter monopile foundations mainly relies on use of the so-called "*p-y*" models, among them the model recommended by API (2014) standard (hereafter referred to as the API *p-y* model) is most commonly adopted in practical design. The applicability of the API *p-y* model to large diameter monopiles with a diameter (D) of 5 to 10m and a small penetration length-to-diameter ratio (L/D) of 5 or less, is debated among the industry and academia. Evidence from centrifuge model testing (Georgiadis et al., 1992; Klinkvort & Hededal, 2014 and Zhu et al., 2016) and numerical simulations (Thieken et al., 2015; Amar Bouzid, 2018 and Wang et al., 2023) suggests that the API *p-y* model severely over-estimates the monopile soil-pile interaction stiffness and capacity in sand. For this reason, alternative solutions are called for. Among others, cone penetration test (CPT) based *p-y* models are attractive as they avoid the uncertainties with derivation of soil parameters which are needed by the spring models, such as the API model and the PISA model (Byrne et al., 2015), either by interpretation of the CPT results or by lab testing of sand samples which are typically performed on reconstituted soil specimens. Several CPT based *p-y* models are available in the literature, such as Novello (1999), Dyson & Randolph (2001), Suryasentana & Lehane (2014, 2016), and Li et al. (2014). However, a thorough examination of the existing CPT-based *p-y* models reveals the following limitations: i) The backbone curves of the models proposed by Novello et al. (1999), Dyson & Randolph (2001), Suryasentana & Lehane (2014) and Li et al. (2014) are power law functions. This function form lacks the capacity to predict the ultimate soil resistance (p_u); ii) Suryasentana & Lehane (2016) designed their model as a piecewise function, with the initial *p-y* stiffness set to $4.5G_{max}$ and the backbone curve as an exponential function. The adjustments improve the prediction of k_{ini} and provide a clear p_u, but the piecewise function lacks simplicity and introduces discontinuities to the predicted *p-y* response.

The purpose of this study is to present a CPT-based *p-y* model for monopile analysis in sand that is able to capture the correct initial soil-pile interaction stiffness and the ultimate capacity. The following work has been performed:

1) A lateral pile load test database is established by collating high-quality field tests from four independent studies;

2) A novel *p-y* model is developed based on a modified hyperbolic formulation using the CPT cone tip resistance q_c as the sole input parameter. The predictive capability of the proposed *p-y* model is demonstrated by back-analysis of the tests from the database.

2 MONOPILE TEST DATABASE

The database includes field pile load tests from Li et al. (2014), Murphy et al. (2018), the PISA project (McAdam et al., 2020; Taborda et al., 2020), and Wang et al. (2022). The profiles of CPT cone tip resistance q_c for the field tests are available from the corresponding references.

The geometric and loading information of the field pile load tests is summarized in Table 1. All piles in Table 1 are hollow steel pipe piles with an elastic modulus E_{pile}=210GPa.

Table 1. Geometric information of the field pile load tests

No.	Test ID	$\boldsymbol{D}$ (m)	$\boldsymbol{t}$ (m)	$\boldsymbol{L}$ (m)	$\boldsymbol{h}$ (m)
Li et al. (2014)					
1~3	Li_1~3	0.340	0.014	2.20~4.35	0.40
Murphy et al. (2018)					
4	Murphy_1	0.245	0.008	1.50	0.40
5~7	Murphy_2~4	0.510	0.010	1.50~3.00	1.00
Wang et al. (2022)					
8~10	Wang_1~3	0.127	0.019	0.75~1.50	0.34
11~13	Wang_4~6	0.169	0.0045	1.00~2.50	0.34
14~16	Wang_7~9	0.273	0.0064	0.75~1.50	0.34
17~19	Wang_10~12	0.457	0.0064	0.75~1.50	0.35
PISA project (McAdam et al., 2020; Taborda et al., 2020)					
20~22	PISA_1~3	0.273	0.007	1.43~2.73	5.00
23~24	PISA_4~5	0.762	0.010	2.27~3.98	10.00
25	PISA_6	0.762	0.025	6.02	10.00
26	PISA_7	2.000	0.038	10.61	9.90

Notes: t (m) is the wall thickness of the pile; L (m) is the embedded length of the pile; h (m) is the loading eccentricity.

3 THE CPT-BASED P-Y MODEL

The current model adopts a modified hyperbolic formulation, which introduces a parameter m that controls the stiffness degradation and a parameter A that acts on the ultimate capacity. The specific form of the proposed p-y model is presented in Eq. (1):

$$p = \frac{y}{\left[\left(\frac{1}{k_{ini}}\right)^m + \left(\frac{y}{Ap_u}\right)^m\right]^{\frac{1}{m}}} \quad (1)$$

where k_{ini} (kPa) is the initial p-y stiffness; p_u (kN/m) is the ultimate soil resistance; m is the stiffness degradation coefficient; A is the ultimate soil resistance adjustment coefficient. The calibration for each model parameter using the collected database is elaborated below.

Regarding the modified hyperbolic p-y formulation as presented in Eq. (1), when the lateral displacement (y) approaches 0, the predicted p-y stiffness k=k_{ini}; when the lateral displacement (y) approaches infinity, the predicted soil resistance p=Ap_u. This is demonstrated in Eq. (2):

$$k_{y\to 0} = \left(\frac{p}{y}\right)_{y\to 0} = \left\{\frac{1}{[(1/k_{ini})^m]^{(1/m)}}\right\} = k_{ini} \quad (2a)$$

$$p_{y\to\infty} = \left\{\frac{y}{\{[y/(Ap_u)]^m\}^{(1/m)}}\right\} = Ap_u \quad (2b)$$

3.1 Initial p-y stiffness k_{ini}

Numerous studies (Di Laora & Rovithis, 2015; Wang et al., 2023) have indicated that the initial stiffness of p-y curves at any given depth is directly correlated to the small-strain shear modulus G_{max} of the soil. The current p-y model adopts a simple relationship between k_{ini} and G_{max} where k_{ini}=4.5G_{max}, as proposed by Di Laora & Rovithis (2015), which is also employed by Suryasentana & Lehane (2016) in their CPT-based p-y model.

For the G_{max}, seismic CPT allows for direct measurement of the cone tip resistance and the small-strain shear modulus by measuring the shear wave velocity (V_s). When in-situ data do not include G_{max}, it is recommended to utilize the empirical relationship between G_{max} and q_c suggested by Baldi et al. (1989) as presented in Eq. (3):

$$G_{max} = \rho_T V_s^2 \quad (3a)$$

$$V_s = 277 q_c^{0.13} (\sigma_v')^{0.27} \quad (3b)$$

where: ρ_T (kg/m^3) is the total soil mass density; V_s (m/s) is the shear wave velocity. The units of q_c and σ_v' are in MPa in Eq. (3).

3.2 Ultimate soil resistance p_u

The soil resistance distribution model proposed by Petrasovits & Award (1972) is employed in this study. Based on this soil resistance distribution as well as the equilibrium of force and moment, the ultimate lateral capacity H_u (kN) and the corresponding ultimate overturning moment capacity M_u (kN·m) at the mudline can be calculated in Eq. (4):

$$H_u + H_b = \int_0^d p_u \mathrm{d}z - \int_d^L p_u \mathrm{d}z \quad (4a)$$

$$M_u + H_b L - M_b = \int_0^d p_u z \mathrm{d}z - \int_d^L p_u z \mathrm{d}z \quad (4b)$$

where H_b (kN) is the shear force at the pile base; M_b (kN·m) is the moment at the pile base; d (m) is the depth of rotation point from the mudline.

According to the field tests by Wang et al. (2022), the effect of base resistance on rigid monopile response is shown to be negligible. Therefore, with Eq. (4), the ultimate lateral loading capacity (H_u and M_u) at the mudline of a rigid pile can be determined if the expression for p_u is known. Based on the ultimate capacities determined from the field pile load tests, the following Eq. (5) for p_u is calibrated:

$$p_u = 0.55Dq_c^{0.7}(\sigma_v')^{0.3} \tag{5}$$

3.3 Adjustment coefficient *m* and *A*

This section presents the calibration of the stiffness degradation coefficient *m* and the ultimate soil resistance adjustment coefficient *A*. The calibration process involves repeatedly adjusting the values of *m* and *A* until the proposed *p-y* model provides the best prediction to the load-displacement curves measured in the field tests of the database. The variation of the best-fit values of *m*, *A* with the *L/D* ratio of the piles covered in the pile load test database is presented in Figure 1.

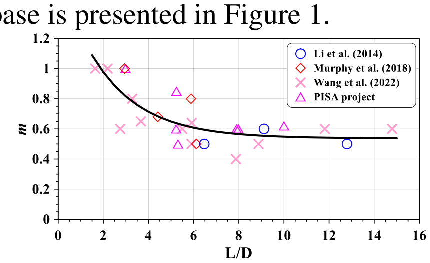

(a) Stiffness degradation coefficient m

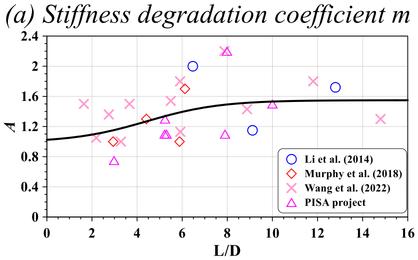

(b) Ultimate soil resistance adjustment coefficient A

Figure 1 The relationship between coefficients m, A and the L/D of piles

In the predictions of the field model test presented in Section 4, the values of coefficients *m* and *A* are determined according to the fitted curves (black solid line) in Figure 1. The explicit formulations of the fitted curves are presented in Eq. (6):

$$m = 0.537 + 1.095 \times 0.633^{L/D} \tag{6a}$$

$$A = 1.549 - \frac{0.560}{1 + e^{(L/D - 4.424)/1.628}} \tag{6b}$$

4 MODEL PREDICTIONS VS. TEST DATA

This section presents an evaluation of the performance of the proposed *p-y* model. The prediction results are compared with the filed test data in Figure 2 to Figure 5. In addition, predictions using the API *p-y* model, the existing proposed CPT-based *p-y* models (Li et al., 2014; Suryasentana & Lehane, 2016), and the PISA model using General Dunirk Sand Model parameters (GDSM, as provided by Plaxis Monopile Designer) are presented in the comparison for the tests performed at Dunkirk testing site as presented in Figure 5. To improve the clarity of graphical presentation, only representative cases from each test site are presented.

It should be noted that the GDSM is calibrated for monopiles with 2<*L/D*<6 and 45%<D_r<90% from numerical analyses using Dunkirk sand soil parameters. However, the *L/D* ratio of piles tested at the Dunkirk site from the PISA project varies from 2.93 to 10 and the D_r of the sand covers a range from 75% to 100% (Taborda et al., 2020). In the predictions with the PISA model using the GDSM parameters, D_r is set to 90% in layers with higher relative densities.

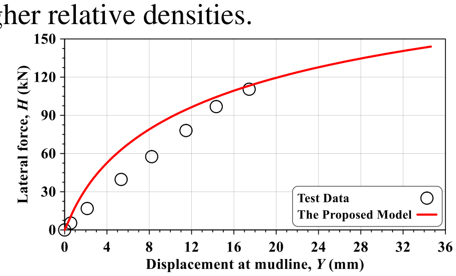

(a) D=0.340m, L=2.20m

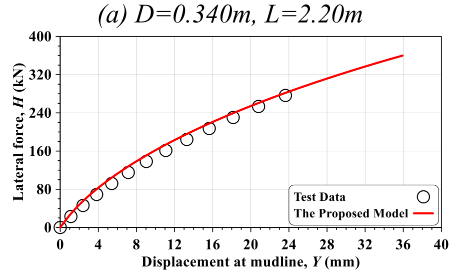

(b) D=0.340m, L=4.35m

Figure 2. The proposed p-y model predictions vs. field pile load tests by Li et al. (2014)

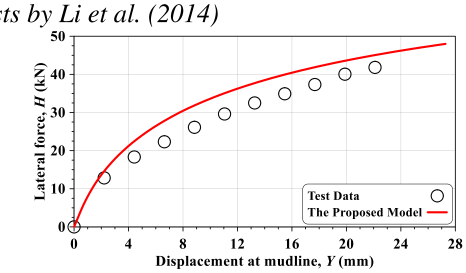

(a) D=0.245m, L=1.50m

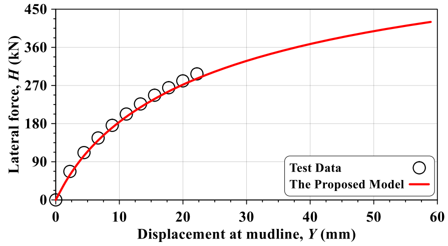

(b) D=0.510m, L=3.00m

Figure 3. The proposed p-y model predictions vs. field pile load tests by Murphy et al. (2018)

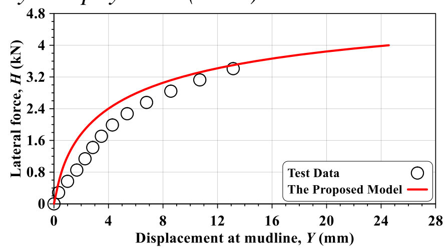

(a) D=0.127m, L=0.75m

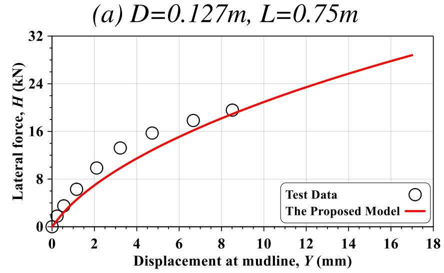

(b) D=0.169m, L=2.50m

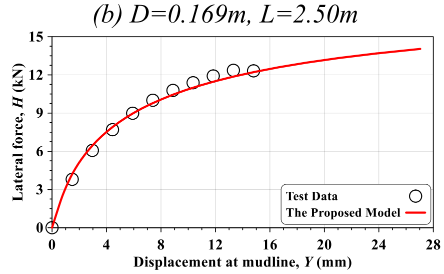

(c) D=0.273m, L=1.00m

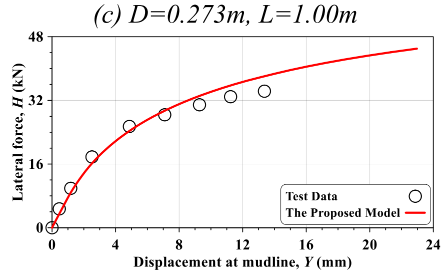

(d) D=0.457m, L=1.50m

Figure 4. The proposed p-y model predictions vs. field pile load tests by Wang et al. (2022)

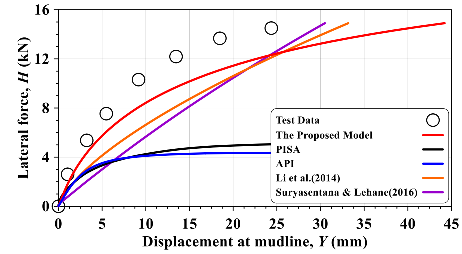

(a) D=0.273m, L=1.43m

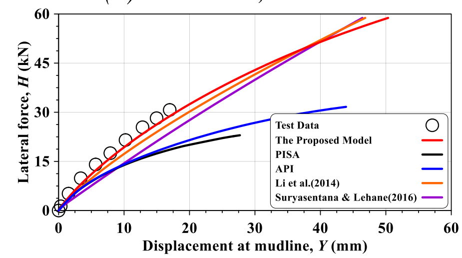

(b) D=0.273m, L=2.73m

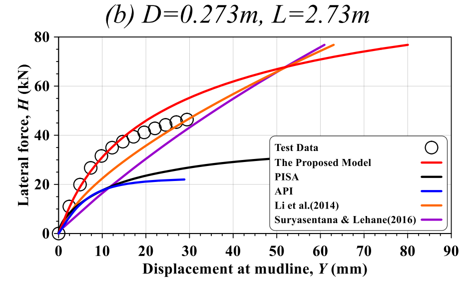

(c) D=0.762m, L=2.27m

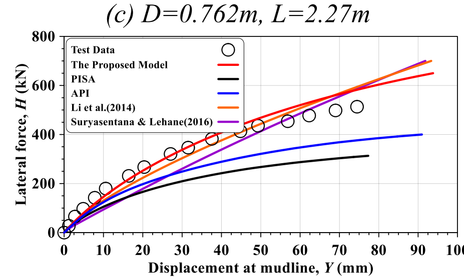

(d) D=0.762m, L=6.02m

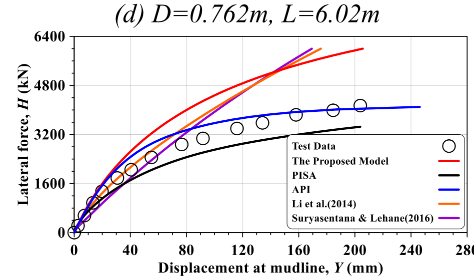

(e) D=2.000m, L=10.61m

Figure 5. The proposed p-y model predictions vs. field pile load tests of the PISA project (McAdam et al., 2020; Taborda et al., 2020)

From the above comparisons in Figure 2 to Figure 5, it is demonstrated that the currently proposed *p-y* model is capable of accurately capturing the soil-pile interaction stiffness for the field pile load tests from four different studies over the full range of lateral displacements that are relevant for practical design.

Furthermore, Figure 5 provides a comparative analysis of the proposed CPT-based *p-y* model against the API model, the PISA model using GDSM parameters, and two existing CPT-based *p-y* models, namely the Li et al. (2014) model and the Suryasentana & Lehane (2016) model. Key observations include:

1) The proposed CPT-based *p-y* model demonstrates superior predictive capability in capturing the initial soil-pile stiffness, while providing acceptable estimation of the pile capacity at larger displacements;

2) The Li et al.(2014) model is shown to present a reasonable prediction to the PISA pile load test despite the initial stiffness is somewhat lower than the test results and the prediction by the currently proposed model. However, due to the power-law function employed by the Li et al. (2014) model, it overtakes the currently proposed model at large displacement as it fails to capture the ultimate capacity of the soil;

3) For the Suryasentana & Lehane (2016) model, although it shares the same k_{ini} as the currently proposed model, k_{ini} is only used for lateral displacements with 0.01%D, beyond which the stiffness is considerably lower. As a result, there is a significant difference in the soil-pile interaction stiffness predicted by the currently proposed model and the model suggested by Suryasentana & Lehane (2016);

4) The API model is shown to understate the soil-pile interaction stiffness and capacity. However, the level of underestimation appears to reduce with the scale of the pile. For the 2 m diameter pile load test, the API model captures the response well. The observation highlights the sensitivity of the API model to stress level and caution should be exercised when the conclusion from small scale field tests is extrapolated to reality. Evidence from centrifuge model tests and numerical simulation generally conclude that the API curves grossly over-estimate the initial stiffness and capacity(e.g., Klinkvort & Hededal, 2014; Thieken et al., 2015; Zhu et al., 2016; Wang et al., 2023);

5) It is somewhat unexpected that the PISA model using the GDSM parameters provides systematically lower predictions in both the initial soil-pile stiffness and ultimate capacity.

CONCLUSIONS

In this study, a novel CPT-based *p-y* model with a modified hyperbolic formulation which contains four model parameters, namely the initial *p-y* stiffness k_{ini}, the ultimate soil resistance p_{u}, the stiffness degradation coefficient m, and the ultimate soil resistance adjustment coefficient A is developed based on a database including 26 high quality field pile load tests from four different studies. Comparisons between the predictions by the proposed *p-y* model with the test data in the database reveal the excellent performance of the model for monopiles of different L/D in sand.

It should be noted that the currently proposed model is calibrated from a still small database of field pile load tests conducted in mainly dense sands with D_{r} ranging from 64% to 100% using relatively small piles with diameter from 0.127m to 2.0m and penetration depth from 0.75m to 10.61m. The following limitations should be considered:

1) Stress level effect. Although the proposed model uses cone tip resistance as input in which the stress level is implicitly considered, the validity of the currently proposed model should still be checked against data obtained from realistic stress levels. While full-scale experiments are prohibitively expensive and impractical if not impossible, considering the extremely high loads involved, one possible approach is to expand the database with centrifuge pile load tests and high-quality numerical simulations. However, a challenge with the centrifuge tests and numerical simulations is that most of them are performed under "wished-in-place" conditions, while the impact installation process is demonstrated to have a large impact on the subsequent lateral pile response in sand (Fan et al., 2021).

2) Small relative density range. The collected field pile load tests in this study concentrate in dense sands with D_{r} greater than 60%, thus the applicability of the currently proposed model to broader relative densities remains unverified.

AUTHOR CONTRIBUTION STATEMENT

Zhentao LIU: Formal Analysis, Writing- Original draft.
Youhu ZHANG: Conceptualization, Supervision.

ACKNOWLEDGMENTS

The authors wish to gratefully acknowledge the financial support by the National Natural Science Foundation of China under Grant No. 52471273.

REFERENCES

Amar Bouzid, D. (2018). Numerical Investigation of Large-Diameter Monopiles in Sands: Critical Review and Evaluation of Both API and Newly Proposed *p-y* Curves. *Int. J. Geomech*, 18(11),04018141.https://doi.org/10.1061/(ASCE)GM.1943-5622.0001204

API, (2014). Recommended Practice 2AWSD Planning, Designing and Constructing Fixed Offshore Platforms-Working Stress Design. American Petroleum Institute.

Baldi, G., Bellotti, R., Lo Presti, D. C. F., Ghionna, V. N., & Jamiolkowski, M. (1989). Modulus of sands from CPT's and DMT's. 12th International Conference on Soil Mechanics and Foundation Engineering, 165–170.

Byrne, B., McAdam, R., Burd, H., et al. (2015). New design methods for large diameter piles under lateral loading for offshore wind applications. In *Third International Symposium on Frontiers in Offshore Geotechnic*, Oslo, Norway,705–710. https://doi.org/10.1201/b18442-96

Burd, H. J., Taborda, D. M. G., Zdravković, L., Abadie, C. N., et al. (2020). PISA design model for monopiles for offshore wind turbines: Application to a marine sand. Géotechnique, 70(11),1048-1066. https://doi.org/10.1680/jgeot.18.P.277

Di Laora, R., & Rovithis, E. (2015). Kinematic Bending of Fixed-Head Piles in Nonhomogeneous Soil. *J Geotech Geoenviron*, 141(4), 04014126. https://doi.org/10.1061/(ASCE)GT.1943-5606.0001270

DNV. (2021). DNV-ST-0126-Support structures for wind turbines. Det Norske Veritas.

Dyson, G. J., & Randolph, M. F. (2001). Monotonic Lateral Loading of Piles in Calcareous Sand. *J Geotech Geoenviron*, 127(4), 346–352. https://doi.org/10.1061/(ASCE)1090-0241(2001)127:4(346)

Fan, S., Bienen, B., & Randolph, M. F. (2021). Centrifuge study on effect of installation method on lateral response of monopiles in sand. International Journal of Physical Modelling in Geotechnics, 21(1), 40–52. https://doi.org/10.1680/jphmg.19.00013

Georgiadis, M., Anagnostopoulos, C., & Saflekou, S. (1992). Centrifugal testing of laterally loaded piles in sand. *Can Geotech J*, 29(2), 207–216. https://doi.org/10.1139/t92-024

Jamiolkowski, M., Lo Presti, D. C. F., & Manassero, M. (2003). Evaluation of Relative Density and Shear Strength of Sands from CPT and DMT. *Soil Behavior and Soft Ground Construction*, 201–238. https://doi.org/10.1061/40659(2003)7

Kim, B. T., Kim, N. K., Lee, W. J. et al. (2004). Experimental Load–Transfer Curves of Laterally Loaded Piles in Nak-Dong River Sand. *J Geotech Geoenviron*, 130(4), 416–425. https://doi.org/10.1061/(ASCE)1090-0241(2004)130:4(416)

Klinkvort, R. T., & Hededal, O. (2014). Effect of load eccentricity and stress level on monopile support for offshore wind turbines. *Can Geotech J*, 51(9), 966–974. https://doi.org/10.1139/cgj-2013-0475

Li, W. C., Igoe, D., & Gavin, K. (2014). Evaluation of CPT-based $P-y$ models for laterally loaded piles in siliceous sand. *Géotechnique Letters*, 4(2), 110–117. https://doi.org/10.1680/geolett.14.00021

McAdam, R. A., Byrne, B. W., Houlsby, G. T., et al. (2020). Monotonic laterally loaded pile testing in a dense marine sand at Dunkirk. *Géotechnique*, 70(11), 986–998. https://doi.org/10.1680/jgeot.18.PISA.004

Murphy, G., Igoe, D., Doherty, P., et al. (2018). 3D FEM approach for laterally loaded monopile design. *Comput Geotech*, 100, 76–83. https://doi.org/10.1016/j.compgeo.2018.03.013

Novello, E., A. (1999). From static to cyclic P–y data in calcareous sediments. In *Proc. 2nd Int. Conf. on Engineering for Calcareous Sediments*, Perth, Australia, 17–27.

Petrasovits, G., & Award, A. (1972). Ultimate lateral resistance of a rigid pile in cohesionless soil. In *Proceedings of the 5th European conference on soil mechanics and foundation engineering*, Madrid, Spain, 3, 407–412.

Suryasentana, S. K., & Lehane, B. M. (2014). Numerical derivation of CPT-based *p–y* curves for piles in sand. *Géotechnique*, 64(3), 186–194. https://doi.org/10.1680/geot.13.P.026

Suryasentana, S. K., & Lehane, B. M. (2016). Updated CPT-based $p-y$ formulation for laterally loaded piles in cohesionless soil under static loading. *Géotechnique*, 66(6), 445–453. https://doi.org/10.1680/jgeot.14.P.156

Taborda, D. M. G., Zdravković, L., Potts, D. M., et al. (2020). Finite-element modelling of laterally loaded piles in a dense marine sand at Dunkirk. *Géotechnique*, 70(11), 1014–1029. https://doi.org/10.1680/jgeot.18.PISA.006

Thieken, K., Achmus, M., & Lemke, K. (2015). A new static p-y approach for piles with arbitrary dimensions in sand. *Geotechnik*, 38(4), 267–288. https://doi.org/10.1002/gete.201400036

Wang, H., Lehane, B. M., Bransby, M. F., et al. (2022). Field and numerical study of the lateral response of rigid piles in sand. *Acta Geotech*, 17(12), 5573–5584. https://doi.org/10.1007/s11440-022-01532-6

Wang, H., Lehane, B. M., Bransby, M. F., et al.(2023). Lateral behavior of monopiles in sand under monotonic loading: Insights and a new simple design model. *Ocean Eng*, 277, 114334. https://doi.org/10.1016/j.oceaneng.2023.114334

Zhu, B., Li, T., Xiong, G., & Liu, J. C. (2016). Centrifuge model tests on laterally loaded piles in sand. *Int J Phys Model Geo*, 16(4), 160–172. https://doi.org/10.1680/jphmg.15.00023